

Phase Transitions in Metastable Fe-Ga Alloys

Igor S. Golovin, Valeria Palacheva,
AbdelKariem Mohamed

Department of Physical Metallurgy of non-Ferrous Metals
National University of Science and Technology "MISIS"
Moscow, Russia

e-mail: i.golovin@misis.ru, lera.palacheva@mail.ru,
abdelkarim.abdelkarim@feng.bu.edu.eg

Anatoliy Balagurov, Ivan Bobrikov,
Natalia Samoylova, Sergei Sumnikov

Frank Laboratory of Neutron Physics
Joint Institute for Nuclear Research
Dubna, Russia

e-mail: bala@nf.jinr.ru, bobrikov@nf.jinr.ru,
rny03@nf.jinr.ru, sumnikovsv@gmail.com

Abstract — In the present study, we have investigated the time and temperature dependence of the transition of as-cast metastable Fe-(9-33at.%)Ga ‘Galfenol’ alloys to the equilibrium state along with corresponding changes in their functional properties and anelastic effects that accompany these transitions. To characterize such a Time-Temperature Transformation (TTT) diagram, we used both long-time isochronal annealing (up to 300hrs) and instant heating treatments with different temperature protocols. In-situ neutron diffraction, X-Ray Diffraction (XRD), Differential Scanning Calorimetry (DSC), Vibrating-Sample magnetometer (VSM), Vickers Hardness (HV), Scanning Electron Microscope-Electron Backscatter Diffraction (SEM-EBSD), Mössbauer and mechanical spectroscopy techniques were used.

Keywords-Fe-Ga; neutron diffraction; phase transitions; equilibrium.

I. INTRODUCTION

Fe-Ga bulk poly- and single crystals, foils and nanowires found various applications with the main emphasis on their enhanced magnetostriction properties. Several important questions about the structure and properties of Fe-Ga alloys remain open: e.g., Jouliau vs. non-Jouliau magnetostriction [1], the origin of different short range ordered clusters and their contribution to properties [2], pseudoelasticity [3], anomalous temperature dependence of Young's modulus [4], damping capacity and anelasticity of phase transitions [5], etc.

The equilibrium phase diagram does not reflect the real structure of Fe-Ga alloys neither in the as-cast state nor after annealing followed by air or furnace cooling [6]. The metastable phase diagram, proposed by Ikeda et al. in 2002 [7], is too general and it corresponds only to the chosen regimes of cooling of Fe-Ga alloys. Functional properties of the Fe-Ga alloys are extremely sensitive to particular details of the phase transition from the metastable (as-cast, as-quenched, air-cooled) state with A2 or short and long range D0₃ ordered structures with positive magnetostriction to the equilibrium state with L1₂ structure and negative magnetostriction [8][9].

The aim of this paper is twofold: it is not only to study both the structure and sequence of phase transitions in

metastable Fe-Ga alloys, but also to examine the rates of the transitions using different techniques, including both *in situ* tests with different heating rates and long-term isothermal annealing treatments. Those characteristics are of high interest and importance in order to design specific microstructures with desired properties.

The rest of the paper is structured as follows: In Section II, we describe the experimental procedure; the results are presented in Section III. Finally, we conclude in Section IV.

II. EXPERIMENTS

The Fe-Ga alloys were produced by induction melting followed by casting in an Indutherm MC-20 V mini furnace under protective high-purity argon gas. The chemical composition of the produced ingots was analysed by Energy Dispersive X-ray Spectroscopy (EDX). The tolerance (± 0.1) comes from the calibration by measuring standard samples with a purity of 99.9999% of element. The standard error of measurement of the chemical composition is 0.1-0.2% wt. In this paper, we use only atomic %.

Neutron Diffraction (ND) patterns were measured with a High-Resolution Fourier Diffractometer (HRFD) operating at the fast pulsed reactor IBR-2 which, is a powerful neutron source at Joint Institute for Nuclear Research Dubna, Russia (JINR). The HRFD can be switched between high-resolution ($\Delta d/d \approx 0.0015$) and high-intensity ($\Delta d/d \approx 0.015$) diffraction modes, both of which are needed for a joint analysis of the changes in the atomic structure and microstructure of the material upon heating or cooling. A detailed description of the method is given in [10], where a comparative analysis of the results obtained on as-cast and powder samples of the Fe-27Ga alloy was carried out. Most of the *in situ* experiments were carried out with heating and cooling rates of 2 °C/min. Some tests were also carried out with cooling rates of 1, 4, 8 °C/min, respectively.

XRD analysis of the crystallographic structure of the samples was performed with a Bruker D8 Advanced diffractometer with Cu K α radiation. The room temperature XRD tests and selected SEM-EBSD tests we used after 300 hrs annealing in vacuum at different temperatures, namely: 300, 350, 400, 450, 500, 575°C, respectively.

Internal Friction (IF), or the loss factor Q^{-1} , were obtained from forced vibrations by measuring the phase lag $\tan\varphi$ between the applied cyclic stress and the resulting strain: $\sigma = \sigma_0 \cos(\omega t)$ and $\varepsilon = \varepsilon_0 \cos(\omega t + \varphi)$, correspondingly. $\omega = 2\pi f$ and φ is the phase lag or the loss angle. The temperature-dependent measurements were conducted as a function of temperature between 0 and 600 °C using forced bending single cantilever vibrations with $\varepsilon_0 = 7 \times 10^{-5}$ with heating and cooling rates of 2 °C/min.

DSC experiments using a Labsys Setaram system with heating rates of 5, 10 and 20 °C/min in air atmosphere allowed us to carry out the sample's thermal analysis.

The dilatometry tests were recorded at temperatures ranging from 20 °C to 800 °C at the heating rate of 5 °C/min using a Dilatometer Linseis L75.

Magnetization (VSM) curves were obtained using a VSM-130 vibrating sample magnetometer with a heating rate of 6 °C/min under a magnetic field of ≈ 400 kA/m.

SEM-EBSD microstructures of the alloys were identified by SEM operating at 20kV using a TESCAN VEGA LMH microscope with a LaB6 cathode and an energy dispersive X-ray microanalysis system (Oxford Instruments, Software Advanced AZtecEnergy). Both backscattered electron and secondary electron imaging were used in the analysis. EBSD analysis of the alloys was investigated using the NordlysMax2 detector (Oxford Instruments, Software Advanced AZtecEnergy) with a Crystal Structure Database supplied by Oxford Instruments. The Mean Angular Deviation (MAD) of 0.25 was used in the analysis.

III. RESULTS

To characterize a TTT diagram, which is isothermal transformation diagram we used long-time isochronal annealing (up to 300 hrs), instant heating and instant cooling treatments with different cooling rates from 1 to 2500 °C/min.

A. As-cast alloy structures at room temperature

According to their structure, the as-cast samples can be divided into four groups:

1. $x < 20$, A2 structure,
2. $20 < x < 27$, A2 as a matrix with $D0_3$ clusters embedded into the matrix (existence of small amount of B2 clusters is also not excluded),
3. $27 < x < 31$, $D0_3$ and B2 structures.
4. $x > 31$, B2 or $D0_3$ plus a phase with unresolved structure.

Within the second group, there are two subgroups:

- 2a. $21 < x < 23$, lattice parameter and width of fundamental peaks decrease,
- 2b. $23 < x \leq 27$, lattice parameter increases linearly while the intensity of superstructure peak (111) increases, reaches maximum, and decreases.

The lattice parameter is more sensitive to the beginning of the ordering process than the peak intensities. Up to $x \approx$

27, the ordered clusters occupy a relatively small volume as compared to the volume of a disordered matrix.

B. Phase transitions at heating of as-cast alloys

Second order phase transition in Fe-19Ga type alloys

Ordering in Fe-19Ga type alloys is studied and confirmed for different regimes of heat treatment of the samples [11]. Transmission electron microscopy study suggests that ordering results in formation of small $D0_3$ type ordered clusters.

In situ neutron diffraction study confirms disordering of Fe-19Ga structure at heating above 400°C and ordering at slow cooling. By means of internal friction and vibrating sample magnetometry measurements, which have high sensitivity to atomic disordering and change in magnetization, ordering temperature (T_0) was determined to be 500-550°C at heating and 525-485°C at cooling. It looks like that doping with Tb enhances this effect, but more careful study is needed in future, as both Tb and Ga concentrations influence on the temperature ordering-disordering reaction and degree of ordering.

First order phase transition in Fe-27Ga type alloys

Using the *in situ* neutron scattering technique (Fig. 1), we have defined ranges of phase transitions in the bulk samples of Fe-Ga alloys with 25 to 28 %Ga under constant heating with the rate 1 and 2 K/min [12][13]. We underline different rates of lattice parameters $a(D0_3)$ and $a(L1_2)$ increases in the temperature range of their co-existing, which lead to an anelastic behaviour of the alloy in this temperature range. Using a combination of neutron scattering technique with heat flow, magnetization, and internal friction tests analyses, we proved that a transient internal friction P_{Tr} peak accompanies the $D0_3$ to $L1_2$ phase transition during heating in a wide range of Ga concentrations [14].

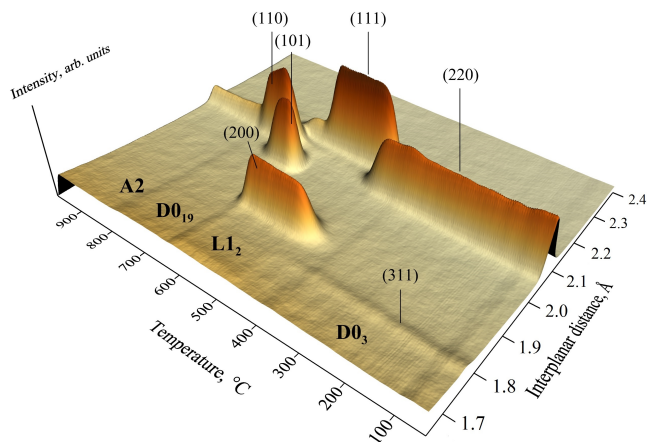


Fig. 1. The 3D visualization of the diffraction peak evolution upon heating the Fe-27Ga sample. The short interplanar distance range around $d = 2$ Å is shown.

C. Phase transitions at isothermal annealing

Isothermal annealing of Fe-(27-28)Ga alloys at 400 to 470 °C leads to the D0₃ → L1₂ phase transition. The analysis of the intensities of the fundamental and superstructure diffraction peaks over time in *in situ* regime reveals that the transition between the ordered structures D0₃ and L1₂ occurs through the formation of the disordered state [15]. In other words, the sequence D0₃ → A2 → A1 → L1₂ is realized, where A1 and A2 are disordered fcc and bcc structures (Fig. 2). The transition process begins with a rather abrupt disappearance of the ordering in the D0₃ phase, i.e. the formation of the A2 bcc structure. Then, the bcc → fcc transformation, apparently via a mechanism like the α → γ transition in pure iron, occurs, followed by the formation of the ordered L1₂ phase. An important difference in the bcc → fcc transition in Fe-xGa alloys at x ~ (27-28) is significantly lower temperature than in pure iron (T_c ≈ 911 °C). As in pure iron, the diffraction patterns for these alloys show no evidence of tetragonal distortion, i.e. the A2 → A1 transition occurs in small local sample volumes in time intervals too short to allow observation of changes in the diffraction pattern.

During disordering (D0₃ → A2) and ordering (A1 → L1₂) transitions, the lattice deformation is homogeneous and very small (ε ≤ 0.001), whereas during the first-order A2 → A1 transition, the linear deformations are heterogeneous and large: ε_c ≈ 0.266, ε_{ab} ≈ -0.105.

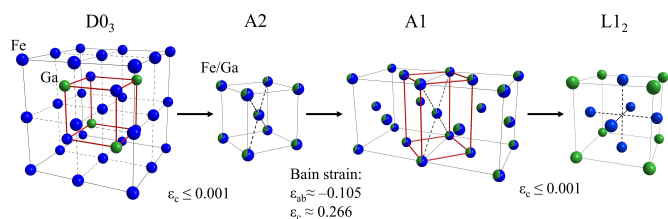


Fig. 2. Schematic diagram of the D0₃ → A2 → A1 → L1₂ structural transitions in the Fe-27Ga type alloys during isothermal annealing. D0₃ and A2 are bcc-based ordered and disordered structures. A1 and L1₂ are fcc-based disordered and ordered structures. The lattice deformation is small for the D0₃ → A2 and A1 → L1₂ transitions and relatively large for the A2 → A1 transition.

The kinetics of the whole transition process cannot be described within the Avrami model [16], since the value of the Avrami parameter *n* does not remain constant with the annealing time. However, it is possible to find out intervals with *n*(*t*) ≈ const. For the initial stage of the transition in Fe-27Ga, the Avrami parameter is close to *n* = 2 for all annealing temperatures between 400 and 470 °C, which corresponds to the model with a constant growth rate of new-phase grains and a decreasing nucleation rate.

D. Long-term (300°C) annealing at 300-575°C

300 hrs annealing in vacuum of as-cast Fe-Ga samples was applied in order to achieve equilibrium state. Our experimental points are added to equilibrium phase diagram [17] based on Gödecke and Köster [18] studies. Each point illustrates the ratio between bcc phase (here we do not

distinguish between A2 and D0₃ structures), fcc-derived L1₂ phase, and R (Fe₆Ga₅) phase. These phases are shown by green, red and blue colours, correspondingly. Our results demonstrate significant deviation from the generally accepted diagram [17]: obviously, the boundary between the A2 and (A2+L1₂) ranges is located at lower Ga content. This observation is in favour of the less known phase diagram suggested by Bras et al. [19]. Nevertheless, both diagrams fail to explain experimental points close to the (A2+L1₂) and L1₂ boundary. We suggest that the range of single A2 phase is more narrow as compared with existing phase diagrams. Also, the results presented in Fig. 3 support a typical C-type of TTT diagram (Fig. 4). 300 hrs annealing at 575, 400, 350 and 300 °C is not enough to complete transition to equilibrium phase, in contrast with annealing at 500 and 450 °C, which are close to the ‘nose’ of the C curve.

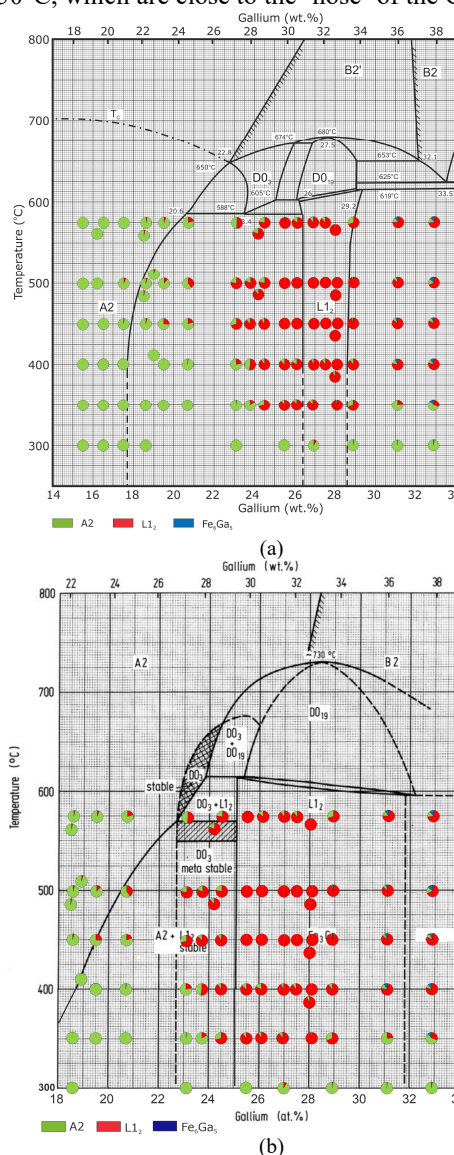


Fig. 3. Fe-Ga equilibrium phase diagrams [16] (a) and [18] (b) with experimental points illustrating the ratio between bcc (A2/D0₃), L1₂ and R (Fe₆Ga₅) phases after 300hrs annealing.

E. Phase transitions at cooling and critical cooling rates

The Fe-27%Ga sample was cooled down from 900°C with well-controlled cooling rates from 1 to 2000 °C/min. Sample structures were examined to identify the first and second critical cooling rates. The scheme of the TTT diagram is shown in Fig. 4. The first critical cooling rate, V_{Cr1} , is defined in this paper as the cooling rate of beginning of the appearance of the equilibrium $L1_2$ phase out from the metastable $D0_3$ phase, and the second critical cooling rate, V_{Cr2} , is the cooling rate at which no metastable phase ($A2$, $B2$ or $D0_3$) is fixed in the sample structure at cooling.

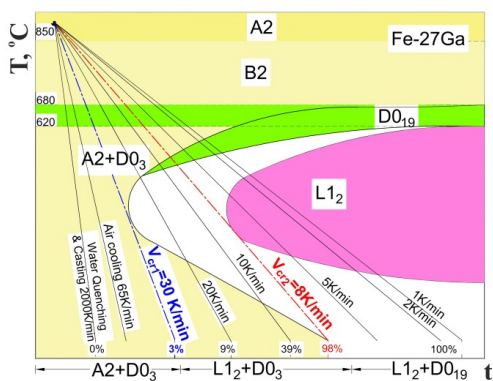


Fig. 4. Scheme of temperature - time transformation (TTT) diagram for Fe-27Ga alloy with two critical cooling rates of 30 and 8 K/min and indication of final structures at room temperature for given cooling rates according to our results.

IV. CONCLUSIONS

In this paper, we have analysed structure in the Fe-(9-33)Ga as-cast alloys and their phase transitions in them at instant heating, short-term *in situ* isothermal and long-term annealing, and phase transitions after annealing in A2 range of phase diagram and subsequent cooling with different rates. Results reveal that the boundary between the A2 and ($A2+L1_2$) ranges is located at lower Ga content and the appearance of $L1_2$ depends on the cooling rate.

ACKNOWLEDGMENT

This work is supported by the Russian Science Foundation (project No. 19-72-20080).

REFERENCES

[1] H. D. Chopra and M. Wuttig, "Non-Joulian magnetostriction." *Nature*, vol. 521, May 2015, pp. 340-343, doi:10.1038/nature14459.
 [2] C. Mudivartha, M. Laver, J. Cullen, A. B. Flatau, and M. Wuttig, "Origin of magnetostriction in Fe-Ga." *Journal of Applied Physics*, vol. 107, May 2010, pp. 09A957, doi:10.1063/1.3359814.
 [3] H. Y. Yasuda, M. Aoki, A. Takaoka, and Y. Umakoshi, "Pseudoelasticity in Fe_3Ga single crystals." *Scripta Materialia*, vol. 53, April 2005, pp. 253-257, doi:10.1016/j.scriptamat.2005.03.032.

[4] M. Li et al., "Anomalous temperature dependence of Young's modulus in $Fe_{73}Ga_{27}$ alloys." *Journal of Alloys and Compounds*, vol. 701, April 2017, pp. 768-773, https://doi.org/10.1016/j.jallcom.2017.01.175.
 [5] I. S. Golovin and J. Cifre, "Structural mechanisms of anelasticity in Fe-Ga-based alloys." *Journal of Alloys and Compounds*, vol. 584, September 2014, pp. 322-326, http://dx.doi.org/10.1016/j.jallcom.2013.09.077.
 [6] I. S. Golovin et al., "Comparative study of structure and phase transitions in Fe-(25-27)%Ga alloys." *Journal of Alloys and Compounds*, vol. 811, November 2019, pp. 152030, https://doi.org/10.1016/j.jallcom.2019.152030.
 [7] O. Ikeda, R. Kainuma, I. Ohnuma, K. Fukamichi, and K. Ishida, "Phase equilibria and stability of ordered b.c.c. phases in the Fe-rich portion of the Fe-Ga system." *Journal of Alloys and Compounds*, vol. 347, December 2002, pp. 198-205, https://doi.org/10.1016/S0925-8388(02)00791-0.
 [8] I. S. Golovin et al., "From metastable to stable structure: the way to construct functionality in Fe-27Ga alloy." *Journal of Alloys and Compounds*, vol. 751, June 2018, pp. 364-369, https://doi.org/10.1016/j.jallcom.2018.04.127.
 [9] I. S. Golovin et al., "Phase transitions in Fe-27Ga alloys: guidance to develop functionality." *Intermetallics*, vol. 100, September 2018, pp. 20-26, https://doi.org/10.1016/j.intermet.2018.05.016.
 [10] A. M. Balagurov, I. S. Golovin, I. A. Bobrikov, V. V. Palacheva, S. V. Sumnikov, and V. B. Zlokazov, "Comparative study of structural phase transitions in bulk and powdered Fe-27Ga alloy by real-time neutron thermodiffraction." *J. Appl. Crystallogr.*, vol. 50, February 2017, pp. 198-210, https://doi.org/10.1107/S1600576716020045.
 [11] I. S. Golovin et al., "In situ studies of atomic ordering in Fe-19Ga type alloys." *Intermetallics*, vol. 105, February 2019, pp. 6-12, https://doi.org/10.1016/j.intermet.2018.10.029.
 [12] I. S. Golovin, A. M. Balagurov, V. V. Palacheva, I. A. Bobrikov, and V. B. Zlokazov, "In situ neutron diffraction study of bulk phase transitions in Fe-27Ga alloys." *Materials and Design*, vol. 98, May 2016, pp. 113-119, https://doi.org/10.1016/j.matdes.2016.03.016.
 [13] I. S. Golovin and A. M. Balagurov, *Structure induced anelasticity in iron intermetallic compounds and alloys*, Materials Research Forum LLC, USA, 2018.
 [14] I. S. Golovin, V. V. Palacheva, J. Cifre, and C. Jiang, "Internal friction in Fe-Ga alloys at elevated temperatures." *Journal of Alloys and Compounds*, vol. 785, May 2019, pp. 1257-1263, https://doi.org/10.1016/j.jallcom.2019.01.265.
 [15] A. M. Balagurov, N. Y. Samoylova, I. A. Bobrikov, S. V. Sumnikov, and I. S. Golovin, "The first and second-order isothermal phase transitions in Fe_3Ga -type functional intermetallic compounds." *Acta Crystallographica Section B: Structural Science, Crystal Engineering and Materials*, vol. 75, 2019, RA5070, in press.
 [16] M. Avrami, "Kinetics of phase change. I General theory." *Journal of Chemical Physics*, vol. 7, 1939, pp. 1103-1112, doi:10.1063/1.1750380.
 [17] O. Kubaschewski, *Iron-binary phase diagrams*, Springer-Verlag, Berlin, 1982.
 [18] T. Gödecke and W. Köster, "Über den aufbau des systems Eisen-Gallium zwischen 10 und 50 at.% Ga und dessen abhängigkeit von der wärmebehandlung." *Z. Metallkde*, vol. 68, 1977, pp. 758-764.
 [19] J. Bras, J.J. Couderc, M. Fagot, J. Ferre, "Transformation ordre-desordre dans la solution solide de fer-gallium." *Acta Metallurgica*, vol. 25, Sept. 1977, pp. 1077-1084, https://doi.org/10.1016/0001-6160(77)90137-7.